

# Influence of manufacturing parameters on the tensile strengths of hollow and solid glass fibres

M. J. HUCKER, I. P. BOND

*Department of Aerospace Engineering, University of Bristol, Queen's Building, University Walk, Bristol BS8 1TR., UK*  
E-mail: *aero-office@bristol.ac.uk*

S. HAQ

*BAE SYSTEMS Advanced Technology Centre - Sowerby, Bristol BS34 7QW, UK,*

S. BLEAY, A. FOREMAN

*DERA Farnborough, Griffith Building, Farnborough, Hants GU14 0LX, UK*

---

Composites reinforced with hollow glass fibres (HGF) have been shown to display improved performance in flexural and compressive loading over materials reinforced with solid fibres. A major drawback associated with hollow fibre composites is reduced reinforcement cross-section for a given fibre volume fraction. It is suggested that the use of optimised manufacturing parameters may allow fibre strengths to be increased, offsetting the inherent strength reduction predicted for hollow fibre composites compared to solid fibre composites. Tensile tests have been performed on batches of hollow and solid fibres with a variety of geometry's to investigate the effects of fibre hollow fraction and manufacturing parameters on fibre strength. Hollow and solid glass fibres drawn under a variety of conditions display tensile strengths which reflect their manufacturing history. A mechanism is proposed whereby differential strains may be locked into the fibre during manufacture. This mechanism may provide an explanation for the strength variations observed. Average tensile strengths for solid and hollow glass fibres appear to increase according to the degree of residual strain differential. The principal manufacturing parameters influencing residual strain differential are draw rate and temperature. Further investigation is suggested into methods for determining heat transport mechanisms within the fibre neck-down zone. © 2002 Kluwer Academic Publishers

---

## 1. Introduction

Composites reinforced with hollow glass fibres (HGF) have been shown to display improved performance over materials reinforced with solid fibres. Performance enhancements include, increased specific flexural rigidity [1–6], improved post-impact performance [7], reduced transmission of thermal and acoustic energy [1, 2] and varied dielectric properties [1, 2, 6, 8]. Use of HGF, either alone or in combination with other fibre types opens up possibilities for producing composites with tailored properties [8]. The void at the centre of the fibre has potential for development as a carrier for a functional core [9–11] and may find applications in “smart” materials research.

As part of ongoing investigations at the University of Bristol, in conjunction with DERA Farnborough and BAE SYSTEMS, a series of tensile tests have been performed on hollow and solid fibres to investigate the effects of hollow fraction ( $K^2$ ) and manufacturing parameters on fibre strength. The fibre manufacturing system in the Department of Aerospace engineering (Fig. 1)

is capable of drawing hollow glass fibres of consistent dimensional quality (Fig. 2) under precise parameter control in quantities suitable for experimental scale composite manufacture [12]. Solid glass fibres are normally believed to show increased tensile strengths with reduced diameter as described by Griffith [13], however, work by Otto [14] highlighted the importance of manufacturing conditions on the observed tensile strengths. More recently workers such as Oh [15] have demonstrated that variations in manufacturing parameters will produce changes in observed fibre strength and Weibull [16] distribution. Miller and Geyling [17] have demonstrated a mechanism whereby differential strains may be locked into the fibre during manufacture and this mechanism provides a possible explanation for the variation in strengths observed. The principal manufacturing parameters influencing observed fibre strength are draw rate and temperature as these directly affect both tension and rate of cooling. It is possible that use of optimised manufacturing parameters may allow fibre strengths to be increased by a significant

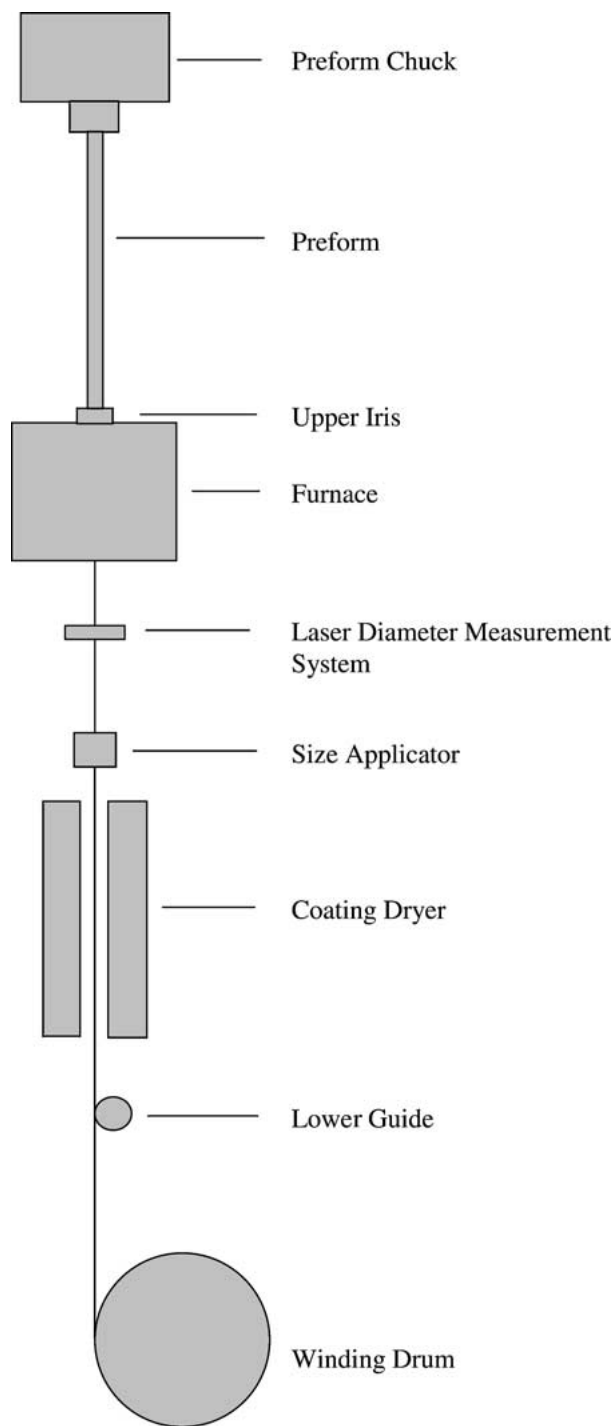


Figure 1 Schematic of fibre drawing tower layout.

margin (e.g 30–70%). This could be used to offset the inherent reduction in tensile strength resulting from the lower cross-sectional area of reinforcement in hollow fibre composites [1, 2, 4].

## 2. Sample preparation

Solid fibres were drawn from circular rods of SIMAX borosilicate glass of 10 mm external diameter (OD). Hollow fibres were drawn from tubular section rods of Schott DURAN glass of 18 mm OD and 15.6 mm internal diameter (ID). Although the two types of preform are from different manufacturers their compositions are almost identical and this is apparent in their physical properties listed in Table I.

TABLE I Composition and physical properties of borosilicate glasses used in manufacture of solid and hollow fibres (Manufacturers data)

Glass type	SIMAX	DURAN
Composition (%Vol.)		
SiO <sub>2</sub>	80.5	81
B <sub>2</sub> O <sub>3</sub>	12.5	13
Al <sub>2</sub> O <sub>3</sub>	2.0	2.0
Na <sub>2</sub> O/K <sub>2</sub> O	4.5	4.0
CaO/MgO	0.5	
Physical properties		
Transformation temperature $T_g/^\circ\text{C}$	540	525
Annealing point/ $^\circ\text{C}$	560	560
Softening point/ $^\circ\text{C}$	825	825
Elastic modulus/GPa	63	64
Poisson's ratio	0.2	0.2
Coefficient of expansion / $^\circ\text{C}$ (20–300 $^\circ\text{C}$ )	$3.3 \times 10^{-6}$	$3.3 \times 10^{-6}$
Density/kg m <sup>-3</sup>	2.23	2.23

TABLE II Fibre drawing parameters

Group	Fibre type	Temperature, $^\circ\text{C}$	Draw rate, ms <sup>-1</sup>	Feed rate, $\mu\text{ms}^{-1}$
A	30/0	1180	1.9	17
B	45/0	1180	1.8	40
C	45/0	1180	1.9	39
D	45/0	1090	1.9	39
E	45/0	1090	3.0	61
F	60/0	1180	1.9	69
G	30/25	1050	1.9	16
H	30/25	1075	2.8	24
I	45/25	1075	1.9	36
J	45/25	1105	3.0	56
K	45/40	1055	1.9	29
L	45/40	1085	2.9	45

Table II gives details of drawing parameters and assigns each group of fibres an identifying letter. The fibre types are listed in the form  $\alpha/\beta$  where  $\alpha$  is the OD in microns and  $\beta$  is the hollow fraction ( $K^2$ ) expressed as a percentage. Fibre hollow fraction is derived from the ratio of core volume per unit length to total volume per unit length as shown in Equation 1.

$$K^2 = \frac{ID^2}{OD^2} \quad (1)$$

Furnace temperatures were measured using a type N thermocouple probe inserted through a ceramic plug mounted in the upper furnace iris (Fig. 1). Temperature data shown are taken at a depth of 150 mm from the top of the furnace. This depth corresponds to the centre of the heating zone. The fibre was wound at a coarse pitch (typically 0.5–1 mm spacing) onto a clean HDPE drum of 340 mm diameter.

## 3. Test procedure

Forty randomly selected sections of each type of fibre were removed from the winding drum and fixed using cyanoacrylate to test cards with a gauge length of 50 mm. All precautions possible were taken to minimize accidental damage during handling, gloves were worn throughout the fibre mounting and testing procedure and care was exercised not to touch the gauge

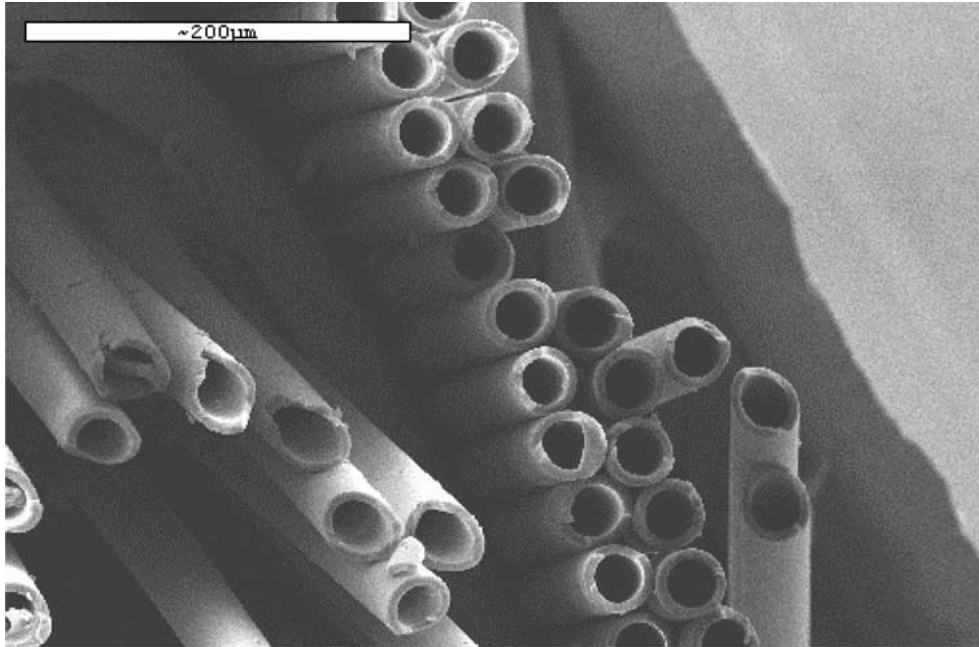


Figure 2 Scanning electron micrograph of 30  $\mu\text{m}$  OD 50% hollow fibres.

length during preparation. Any fibre sections seen to make contact with other fibres were rejected. All testing was carried out between 2 and 3 hours after fibre manufacture to ensure that age effects were minimized. Fibres were tested using a Hounsfield test machine fitted with a 5 N load cell at a rate of  $0.01 \text{ mm s}^{-1}$  according to the ASTM D3379-75 test method.

#### 4. Results

The results from tensile testing are shown in Table III. Fibre external diameter ( $OD_f$ ) was measured continuously during manufacture using a laser diameter measurement system which allowed control to within  $\pm 0.5 \mu\text{m}$  of the desired value. Fibre internal diameter ( $ID_f$ ) was calculated from manufacturing parameters by the method outlined below. It may be reasonably assumed that when fibre is drawn in a stable state it is necessary for the volume flow of material ( $Q$ ) to be equal at all times. If this is the case then the volume flow of preform into the furnace ( $Q_p$ ) equals the volume flow of fibre ( $Q_f$ ) onto the winding drum.

If  $OD_p$ ,  $ID_p$ ,  $V_p$ ,  $OD_f$ ,  $ID_f$ , and  $V_f$  are the preform external diameter, preform internal diameter, preform feed rate, fibre external diameter, fibre internal diameter and fibre draw rate respectively we can write,

$$Q_p = \frac{\pi}{4}(OD_p^2 - ID_p^2)V_p \quad (2)$$

and

$$Q_f = \frac{\pi}{4}(OD_f^2 - ID_f^2)V_f \quad (3)$$

As volume flow is constant during stable state drawing,

$$Q = Q_p = Q_f \quad (4)$$

therefore,

$$ID_f = \sqrt{OD_f^2 - \left( \frac{[OD_p^2 - ID_p^2]}{V_f} V_p \right)} \quad (5)$$

Comparison with values obtained by analysis of optical microscopy images have shown that calculation of

TABLE III Data from fibre tensile testing.  $R^2$  values are for linear fits to the Weibull plots

Group	Ave. tensile strength, MPa	Standard deviation, MPa	Weibull strength, $\sigma_0$ , MPa	Weibull modulus, $M$	$R^2$ value for Weibull plot
A	413.38	38.36	431.04	11.67	0.90
B	363.56	27.61	376.73	13.85	0.96
C	383.12	32.08	397.71	13.36	0.90
D	405.50	56.07	429.36	8.22	0.92
E	438.76	62.28	465.68	7.80	0.97
F	376.31	26.52	388.61	15.50	0.96
G	399.82	163.10	453.61	2.93	0.67
H	549.19	428.15	620.93	1.50	0.74
I	302.25	49.42	323.01	6.80	0.92
J	269.67	39.91	286.45	7.68	0.93
K	364.62	94.46	401.23	4.46	0.72
L	617.57	193.12	687.50	3.48	0.92

TABLE IV Average hollowness fraction,  $K^2$ , values obtained from analysis of optical microscopy images

Fibre type	Fibre hollowness, $K^2$ (estimated using ) (Equation 5)	$K^2$ (average) measured	Error %
60/50	0.50	0.52	-2
60/25	0.25	0.27	-2
45/40	0.40	0.46	-6
45/25	0.25	0.29	-4
30/25	0.25	0.27	-2

$ID_f$  by this method is generally accurate to within 6% (Table IV) and justify the use of the constant volume flow rate assumption.

Draw tension ( $\sigma_f$ ) for the fibres tested here was approximated by the following method. It is assumed that viscous flow occurs at constant volume and under this condition Poisson's ratio  $\nu = 0.5$  and elastic modulus,  $E = 3*G$  (shear modulus) so that the viscosity coefficient ( $\eta$ ) in extension is three times that in shear. The draw tension in the fibre ( $\sigma_f$ ) produced by a given rate of extension ( $\dot{\epsilon}$ ) during viscous flow can then be estimated as follows [19].

$$\sigma_f = 3 \eta \dot{\epsilon} \quad (6)$$

The rate of extension may be derived by dividing the difference of draw rate ( $V_f$ ) and feed rate ( $V_p$ ) by the length of preform entering the furnace in one second ( $V_p$ ).

$$\dot{\epsilon} = \frac{(V_f - V_p)}{V_p} \quad (7)$$

Assuming that the majority of viscous flow occurs at the hottest point in the furnace, i.e. at 150 mm depth,

then an estimation of the viscosity coefficient at this point will allow an approximate value for draw tension to be derived. The radial viscosity coefficient profile in the preform at the start of the hot zone is assumed to have a constant value as the preform feed rates involved are slow enough to allow the material to reach thermal equilibrium. The temperature profile of the furnace near the hot zone has been measured and is approximately linear over the range of temperatures used during manufacture (Fig. 3). The relationship between temperature and viscosity coefficient was estimated by curve fitting manufacturers data (Fig. 4), this yielded the relationship,

$$y = 353285T^{-1.6297} \quad (8)$$

where  $y$  is the viscosity coefficient in  $\log(\text{Pa s})$  and  $T$  is the temperature in  $^{\circ}\text{C}$ . The absolute values of draw tension generated in this manner are not reliable, being based on several approximations. However their relative values do allow some association to be made between draw tension and fibre strength. Table V shows the relationship between approximate drawing tension and average fibre strength.

## 5. Discussion

### 5.1. Solid fibres

Table III shows that the values for 30, 45 and 60  $\mu\text{m}$  OD fibres drawn at  $1.9 \text{ m s}^{-1}$  and  $1180^{\circ}\text{C}$  (Groups A, C and F respectively) display the familiar pattern of lower tensile strength with increasing fibre diameter. The equipment and techniques used allow hollow and solid fibres of identical size to be manufactured under a variety of conditions. The size effect was upset when non-identical drawing conditions were used. Groups

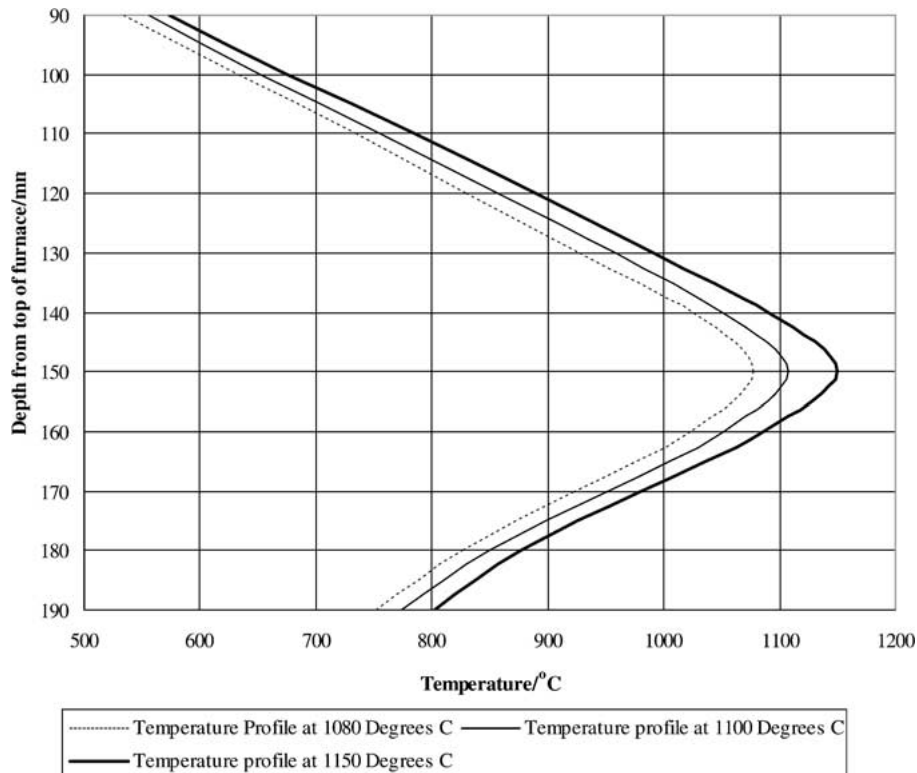


Figure 3 Furnace temperature profile over a range of temperatures.

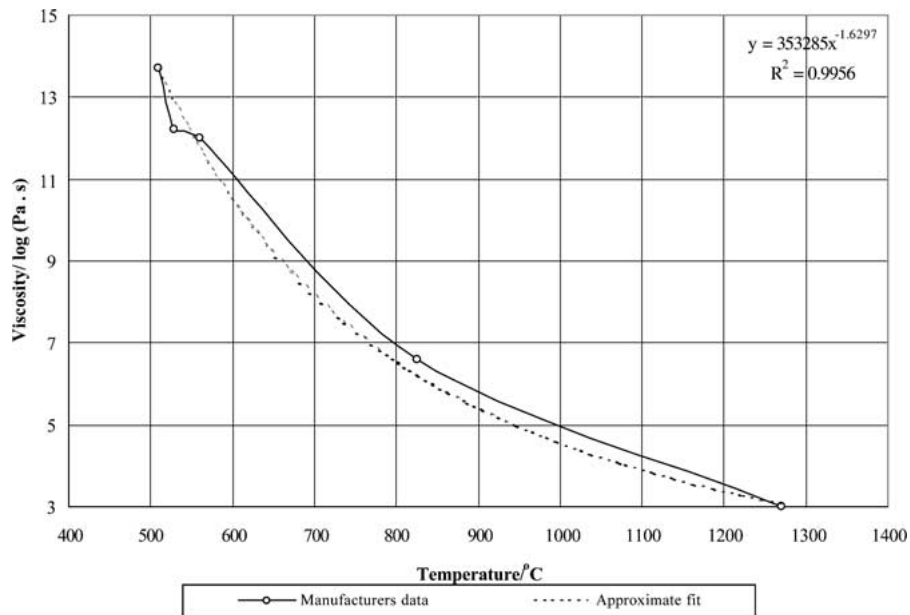


Figure 4 Relationship between temperature and viscosity coefficient derived from manufacturers data.

TABLE V Comparison of average tensile strength with estimated draw tension

Group	Estimated viscosity coefficient ( $\eta$ ), Pa.s	Average tensile strength, MPa	Estimated rate of strain, $s^{-1}$	Draw tension, MPa
A	3037	413.38	111763	1018.2
B	3037	363.56	44999	409.95
C	3037	383.12	48716	443.82
D	9185	405.50	48716	1342.4
E	9185	438.76	49179	1355.1
F	3037	376.31	27535	250.85
G	16295	399.82	118749	5804.9
H	11313	549.19	116665	3959.5
I	11313	269.67	52776	1791.2
J	7512	302.25	53570	1207.3
K	15120	364.62	65516	2971.9
L	9837	617.57	64443	1901.8

of 45/0 fibres were tested to investigate this behaviour (Groups B, C, D and E). Reducing the draw rate had the effect of decreasing the observed strength of the fibres whilst reducing temperature had the opposite effect and strength increased. Combining both of these factors by drawing at high speed and low temperature resulted in group E having an average strength in excess of that observed for the 30  $\mu\text{m}$  OD group A fibres. The degree of scatter increased with average strength, however, the Weibull distributions remained approximately unimodal.

The cooling rate for fibres of this size is very rapid, but there is still a possibility for a significant thermal gradient to exist across the radius of the fibre. It is possible, therefore, that this thermal gradient alone can lead to some degree of toughening by developing a residual compressive stress in the surface layers of the fibre upon cooling (Fig. 5). In addition to this effect it has been shown that the axial velocity of material in the neck-down region is not constant across the fibre radius [17, 20]. In the cooled fibre the drawing stress is constant, so the stress transferred to the neck-down

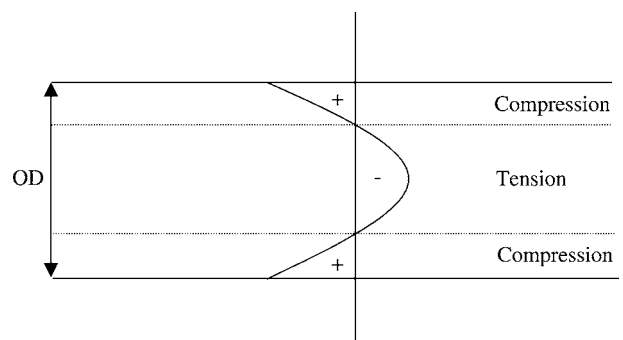


Figure 5 Distribution of thermally induced residual stresses across a fibre.

region will also be constant across the fibre radius. Below the hottest point of the furnace the glass begins to cool, the outside layers cooling more rapidly than the material in the core. This radial temperature gradient results in variation in viscosity coefficient, which with constant applied stress, produces a variation in axial velocity across the fibre. It is suggested that the contraction of the highly strained core material during cooling develops a compressive stress in the already cold, less strained, surface layers of the fibre. It may be argued that shorter flaw lengths will be affected to a greater extent by a compressive stress gradient that increases towards the surface layers of a fibre. If this proves to be the case, then the failure stress distribution may be expected to show a bias towards higher failure stresses. This effect is demonstrated in Fig. 6 where data are plotted for 45/0 fibres at the extremes of the parameters investigated. The values for group E show higher overall values and a distinct change in gradient compared with the those of group B. For the fibres in group E the lower furnace temperature results in higher overall viscosity coefficients and raises the draw tension, likewise the faster draw rate also increases draw tension. By this argument it can be shown that, for solid fibres at least, there is a strong relationship between increased

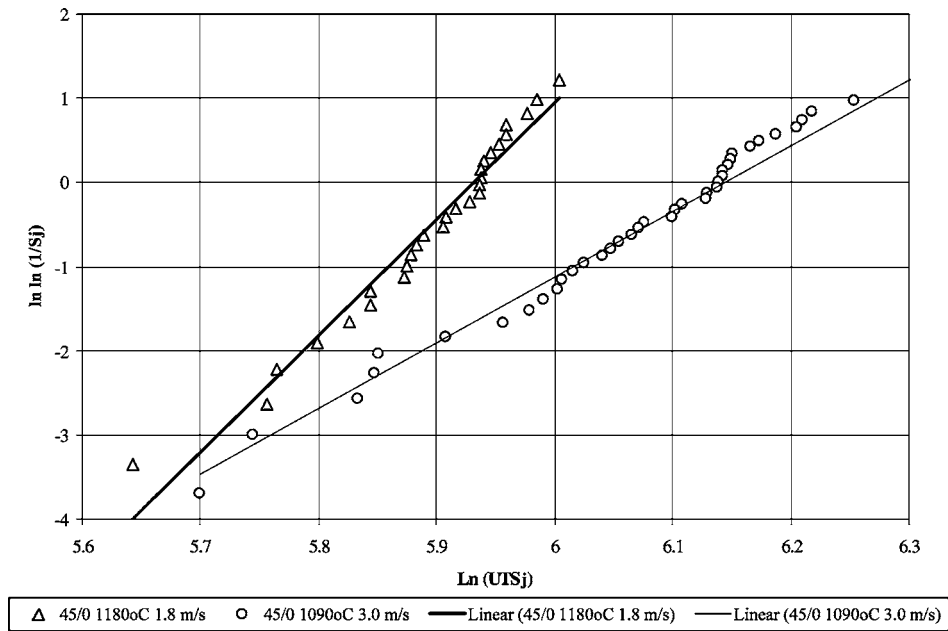


Figure 6 Weibull plot for groups B and E which show a general shift to higher failure stress and biasing towards higher values when draw rate is increased and temperature reduced.

draw tension and higher average fibre strengths and the experimental data appear to confirm this behaviour.

## 5.2. Hollow fibres

Analysis of data from tests on hollow glass fibres is complicated by the nature of the manufacturing process. It is not possible to decouple the drawing parameters, as was done for solid fibres, because the final dimensions depend on a combination of temperature, feed and draw rates. A study of the data in Tables II and III for 30/25 (type G and H), 40/25 (type I and J) and 45/40 (type K and L) fibres shows an average tensile strength change of +37%, -12% and +69% respectively when temperature and draw rate are increased.

The resulting tensile strengths of hollow fibres in this investigation may be explained if one considers that changes in wall thickness, temperature and draw rate all contribute to the viscosity coefficient gradient between the outer and inner fibre wall. As discussed above, differential strains across the fibre radius appear to have a positive effect on ultimate tensile stress. However, on the negative side, if the external layers of the fibre wall are in compression then for equilibrium the surface layers of the inner fibre wall must be in tension. Surface tensile layers would, under normal circumstances, reduce the critical flaw length or lower the critical stress resulting in much weaker fibres. In a hollow fibre the inner wall is, in practical terms, immune from mechanical damage and so may remain in a relatively pristine state and thereby retain a larger proportion of its tensile strength.

The axial velocity gradient across the thickness of the fibre wall is dependent on the drawing tension and on the viscosity coefficient profile. These factors in turn depend on the thermal profile across the fibre wall and how it varies throughout the whole neck-down region. The heat transfer coefficients have been shown to be extremely difficult to estimate in such a dynamic envi-

ronment [17]. It is also difficult to predict the amount of residual strain resulting from the difference in axial velocity. It may be possible, however, to gain some insight into the observed behaviour by comparing the difference between strain rates at the external and internal walls for two fibres under estimated conditions. If we consider two fibres,  $f_1$  and  $f_2$ , with identical dimensions drawn under differing conditions we can estimate draw tension ( $\sigma_d$ ) for the two fibres from the extension rate ( $\dot{\epsilon}$ ) and viscosity coefficient at the external surface ( $\eta_{out}$ ) as follows.

For fibre  $f_1$ ;

$$\sigma_{d1} = 3\eta_{out1} \dot{\epsilon}_1 \quad (9)$$

For fibre  $f_2$ ;

$$\sigma_{d1} = 3\eta_{out2} \dot{\epsilon}_2 \quad (10)$$

The difference between viscosity coefficients ( $\eta_d$ ) at the inner ( $\eta_{in}$ ) and outer ( $\eta_{out}$ ) fibre wall for fibre  $f_1$  and  $f_2$  respectively can be given by,

$$\eta_{d1} = \eta_{out1} - \eta_{in1} \quad (11)$$

and

$$\eta_{d2} = \eta_{out2} - \eta_{in2} \quad (12)$$

So the difference in strain rates ( $\dot{\epsilon}_{diff}$ ) between the internal and external walls for either fibre can be given by,

$$\dot{\epsilon}_{diff} = \frac{\sigma_d}{3\eta_{in}} - \frac{\sigma_d}{3\eta_{out}} \quad (13)$$

To compare  $f_1$  to  $f_2$  we can calculate the ratio of rate of strain differences ( $\dot{\epsilon}_{12}$ ) for the two fibres.

$$\dot{\epsilon}_{12} = \dot{\epsilon}_{diff1} / \dot{\epsilon}_{diff2} \quad (14)$$

Writing Equation 14 in terms of applied stress ( $\sigma_d$ ), the viscosity coefficient difference ( $\eta_d$ ) and the viscosity coefficient at the outer wall ( $\eta_{out}$ ) for the two fibres gives,

$$\varepsilon_{12} = \frac{\sigma_{d1}(\eta_{d1}[\eta_{out2}(\eta_{out2} - \eta_{d2})])}{\sigma_{d2}(\eta_{d2}[\eta_{out1}(\eta_{out1} - \eta_{d1})])} \quad (15)$$

Using Equation 15 the two fibres may be compared. Making the assumption that similar behaviour to that observed for the solid fibres is applicable to hollow fibres, larger residual differential strains may result in higher tensile strengths. Thus if  $\varepsilon_{12} \leq 1$ ,  $f_2$  should be stronger and if  $\varepsilon_{12} \geq 1$ ,  $f_1$  should be stronger.

Other factors such as draw velocity may also affect the viscosity gradient across the fibre wall by altering the rate of cooling. Given the difficulty in obtaining values for heat transfer coefficients it may not be possible at the present time to fully describe the behaviour of the hollow fibres. However, Equation 15 does outline the strong dependence of tensile strength on manufacturing parameters. Further work will attempt to use FEA modelling techniques to predict the heat transfer characteristics and thus allow derivation of residual strains which result from the drawing process.

The hollow fibres tested showed that higher draw tension, higher viscosity and low draw rate resulted in higher strength fibres. On comparing these observations with Equation 15, it is apparent that both the magnitude of viscosity gradient and its absolute values can decide the effect that draw tension has on the residual stress state. It is also the case that size and volume will play a part in fibre strength, although contributions by these factors may be masked by thermally induced stresses as with the solid fibres.

## 6. Conclusions

Hollow and solid glass fibres drawn under a variety of conditions display tensile strengths which reflect their manufacturing history. Average tensile strengths for solid and hollow glass fibres appear to increase according to the degree of residual strain differential. Compressive stresses developed in surface layers of the fibres are likely to be the cause of the observed strengthening. The degree of scatter in tensile strength values increases with tensile strength. Strength increases produced in this way can overcome the expected size effect. The behaviour of hollow glass fibres is strongly dependant on manufacturing history. Further work using FEA techniques is needed to estimate thermal transport mechanisms within the neck-down region especially those mechanisms relating to heat transfer across the fibre wall. Better understanding of the whole process may offer potential to optimise drawing parameters to maximize tensile strength of hollow fibres and thus

offset the reduced fibre volume fraction in a composite material utilising this type of reinforcement.

## Acknowledgements

The authors would like to thank BAE SYSTEMS Advanced Technology Centre - Sowerby, DERA Farnborough and the EPSRC for their financial support of this project via a CASE studentship. This investigation was funded by the MoD under Corporate Research Package TG04.

© British Crown copyright 2000. Published with the permission of the Defence Evaluation and Research Agency on behalf of the Controller of HMSO.

## References

1. B. W. ROSEN, Final Report-15th June 1963-15th August 1964, U.S. Navy, Bureau of Naval Weapons, Contract No.: NOW-63-0674-c (General Electric Missile and Space Division, General Electric company, Philadelphia, PA, 1964).
2. B. W. ROSEN, A. E. KETLER and Z. HASHIN, Final Report, U.S. Navy, Bureau of Naval Weapons, Contract No.: NOW-61-0613-d, (General Electric Missile and Space Division, General Electric company, Philadelphia, PA, 1962).
3. R. F. SIEFERT, *The Glass Industry* June (1963) 321.
4. J. A. BURGMAN, in Symposium on Polymers in Construction, Atlantic City, September 12–17, 1965 (American Chemical Society, 1965).
5. G. NIEDERSTADT, M. GADKE and H. BAUML, in Report No. DLR-FB 76-45 (Deutsche Forschungs- und Versuchsanstalt für Luft- und Raumfahrt, Institut für Flugzeugbau, Braunschweig, 1976).
6. S. A. SCHUSTER and D. R. HARTMAN, in "Dielectric and Structural Properties of HOLLEX™ Fiber Composites" (Owens Corning, Toledo, Ohio, 1993).
7. L. BONIFACE, A. FOREMAN and S. HITCHEN, in Proceedings of the 4th International Conference on Deformation and Fracture of Composites, UMIST 24-26 March 1997 (Institute of Materials, 1997) p. 39.
8. S. M. BLEAY and L. HUMBERSTONE, *Comp. Sci. and Tech.* **59** (1999) 1321.
9. G. F. TAYLOR, *Physics Review* **23** (1924) 655.
10. J. D. AYERS, *J. Mater. Sci.* **28** (1993) 2337.
11. R. LAVIN and I. LEE, in M. Eng. Project report No. 914 (University of Bristol Department of Aerospace Engineering, 2000).
12. M. HUCKER, I. BOND, A. FOREMAN and J. HUDD, *Advanced Comp. Letters* **8** (1999) 181.
13. A. A. GRIFFITH, *Phil. Trans. Royal Soc. of London* **A221** (1921) 163.
14. W. H. OTTO, *J. Amer. Ceram. Soc.* **38** (1955) 122.
15. P. S. OH, J. J. MCALARNEY and D. K. NATH, *ibid.* **65** (1983) C-84.
16. W. WEIBULL, *J. Appl. Mech.* Sept. (1951) 293.
17. T. J. MILLER and F. T. GEYLING, *J. Lightwave Technology* **LT-2** (1984) 349.
18. U. C. PAEK, *ibid.* **4** (1986) 1048.
19. J. ZARZYCKI, "Glasses and the Vitreous State" (Cambridge University Press, Cambridge, 1991) p. 243.
20. H. R. CLARK and M. VIRIYAYUTHAKORN, *J. Lightwave Technology* **LT-4** (1986) 1039.

Received 14 December 2000  
and accepted 3 August 2001